Earth and Planetary Science Letters 389 (2014) 200–208

Contents lists available at ScienceDirect

Earth and Planetary Science Letters

www.elsevier.com/locate/epsl

Decreased influence of Antarctic intermediate water in the tropical Atlantic during North Atlantic cold events

Kuo-Fang Huang [a,b,*], Delia W. Oppo [a], William B. Curry [a,c]

[a] Department of Geology and Geophysics, Woods Hole Oceanographic Institution, Woods Hole, MA, USA
[b] Institute of Earth Sciences, Academia Sinica, Taipei, Taiwan
[c] Bermuda Institute of Ocean Sciences, Bermuda

ARTICLE INFO

Article history:
Received 5 August 2013
Received in revised form 19 December 2013
Accepted 23 December 2013
Available online 15 January 2014
Editor: J. Lynch-Stieglitz

Keywords:
Nd isotopes
Antarctic intermediate water
Atlantic meridional overturning circulation
deglacial variability
North Atlantic cold events

ABSTRACT

Antarctic Intermediate Water (AAIW) is a key player in the global ocean circulation, contributing to the upper limb of the Atlantic Meridional Overturning Circulation (AMOC), and influencing interhemispheric heat exchange and the distribution of salinity, nutrients and carbon. However, the deglacial history of AAIW flow into the North Atlantic is controversial. Here we present a multicore-top neodymium isotope calibration, which confirms the ability of unclean foraminifera to faithfully record bottom water neodymium isotopic composition (ε_{Nd}) values in their authigenic coatings. We then present the first foraminifera-based reconstruction of ε_{Nd} from three sediment cores retrieved from within modern AAIW, in the western tropical North Atlantic. Our records reveal similar glacial and interglacial contributions of AAIW, and a pronounced decrease in the AAIW fraction during North Atlantic deglacial cold episodes, Heinrich Stadial 1 (HS1) and Younger Dryas (YD). Our results suggest two separate phases of reduced fraction of AAIW in the tropical Atlantic during HS1, with a greater reduction during early HS1. If a reduction in AAIW fraction also reflects reduced AMOC strength, this finding may explain why, in many regions, there are two phases of hydrologic change within HS1, and why atmospheric CO_2 rose more rapidly during early than late HS1. Our result suggesting less flow of AAIW into the Atlantic during North Atlantic cold events contrasts with evidence from the Pacific, where intermediate-depth ε_{Nd} records may indicate increased flow of AAIW into the Pacific during the these same events. Antiphased ε_{Nd} behavior between intermediate depths of the North Atlantic and Pacific implies that the flow of AAIW into Atlantic and Pacific seesawed during the last deglaciation.

1. Introduction

The Atlantic Meridional Overturning Circulation (AMOC), the system of warm-to-cold water transformation that results in North Atlantic Deep Water (NADW) production, influences the large-scale redistributions of heat, nutrients, salt and carbon, and therefore has a major influence on Earth's climate system (e.g. Dahl et al., 2005; Zhang and Delworth, 2005 and references therein). Antarctic Intermediate Water (AAIW) is a major contributer to the "cold water" return pathway (e.g., Schmitz Jr. and McCartney 1993), supplying North Atlantic waters that are exported at depth (Rintoul, 1991), and variations in its northward extent in the Atlantic may reflect the strength of the AMOC (Came et al., 2008; Xie et al., 2012; Oppo and Curry, 2012). AAIW also provides an important source of nutrients and carbon to the North Atlantic (Palter and Lozier, 2008) and is an effective sink of anthropogenic CO_2 (Sabine et al., 2004). Nevertheless, deglacial variability of Atlantic AAIW is uncertain; few if any studies have been conducted on sediment cores from within modern Atlantic AAIW, and proxy interpretation of existing data is controversial, with some studies suggesting a smaller fraction of AAIW in the North Atlantic during North Atlantic cold event (Came et al., 2008; Xie et al., 2012) and others arguing for a greater fraction (e.g. Pahnke et al., 2008; Pena et al., 2013).

Nutrient-proxies ($\delta^{13}C$ and Cd/Ca) suggest that the Atlantic deep watermass distribution has varied on glacial–interglacial and shorter time scales (Duplessy et al., 1988; Curry et al., 1988; Boyle and Keigwin, 1987). Many studies suggest that during the Last Glacial Maximum (LGM), high-nutrient (high-Cd, low-$\delta^{13}C$) southern ocean waters made up a greater fraction of deep waters in the North Atlantic below ~2–3 km (e.g. Curry and Oppo, 2005; Marchitto and Broecker, 2006; Lynch-Stieglitz et al., 2007; Yu et al., 2008). $\delta^{13}C$ and Cd reconstructions also suggest a reduced proportion of northern source waters at depth during the two cold North Atlantic deglacial iceberg discharge events,

* Corresponding author at: Institute of Earth Sciences, Academia Sinica, 128, Sec. 2, Academia Road, Nangang, Taipei 11529, Taiwan. Tel.: +886 2 2783 9910x616; fax: +886 2 2783 9871.
E-mail addresses: kfhuang@earth.sinica.edu.tw, kfhuang05@gmail.com (K.-F. Huang).

http://dx.doi.org/10.1016/j.epsl.2013.12.037

Heinrich Stadial 1 (HS1: ~17.5–14.7 kyr Before Present, B.P.) and the Younger Dryas (YD: ~12.8–11.7 kyr B.P.) (Boyle and Keigwin, 1987; Keigwin and Lehman, 1994). Sedimentary radionuclide (^{231}Pa/^{230}Th) records (McManus et al., 2004; Gherardi et al., 2009) suggest that AMOC strength was similar during the LGM and Holocene, but weaker during the North Atlantic deglacial cold events. Taken together, these paleo-records imply a link between nutrient distribution and AMOC strength during the deglaciation. However, variations in the distribution of nutrient proxies are also influenced by contributions of remineralized organic matter remineralization (Kroopnick, 1980) or source water end-member values (e.g., Mix and Fairbanks, 1985), and sedimentary ^{231}Pa/^{230}Th may be influenced by biogenic silica fluxes (Chase et al., 2002). As a result of these potential complications, and to confirm the link between deglacial AMOC variability and global climate change (e.g., Vellinga and Wood, 2002; Lewis et al., 2010), other water mass tracers and circulation proxies must be explored. Among these, neodymium isotopes (ε_{Nd}) measured on unclean planktonic foraminifera hold significant promise, as they appear to record the ε_{Nd} of bottom water (Roberts et al., 2010; Piotrowski et al., 2012; Roberts et al., 2012; Tachikawa et al., 2013); seawater ε_{Nd} is a quasi-conservative water mass tracer within the Atlantic basin (Goldstein and Hemming, 2003).

Here, we test the hypothesis that, as AAIW is an important return flow of NADW that is exported at depth (Rintoul, 1991), its flow into the North Atlantic should, to a large extent, follow variations in the strength of the AMOC (Came et al., 2008; Xie et al., 2012; Oppo and Curry, 2012) as inferred from (^{231}Pa/^{230}Th) records (McManus et al., 2004; Gherardi et al., 2009).

In the Atlantic, southern source waters have high ε_{Nd} values (AAIW: ~−8 to −9; Antarctic Bottom Water, AABW: ~−9; Jeandel, 1993; Stichel et al., 2012) compared to NADW (~−13 to −14) (Piepgras and Wasserburg, 1987). These values reflect the different ages and compositions of the continental crust surrounding the Pacific and Atlantic Oceans, and the mixing ratio between Atlantic and Pacific water masses in the Southern Ocean. Modeling results indicate that boundary exchange is a critical process that helps reconcile the decoupling of Nd concentration and isotopic composition in the ocean (known as the "Nd paradox"; Siddall et al., 2008; Arsouze et al., 2009). Rempfer et al. (2012) further evaluated the potential effect of changes in overturning circulation on seawater ε_{Nd} by applying periodic freshwater fluxes to the North Atlantic and Southern Oceans, and concluded that variations in ε_{Nd} reflect the strength of the formation of NADW and to a greater extent, of AABW. They also concluded that changes in end-member ε_{Nd} values on these abrupt time scales should be relatively small.

Recent studies suggest that ε_{Nd} in unclean planktonic foraminifera (i.e. authigenic coatings that precipitate onto planktonic foraminifera after deposition) record bottom water ε_{Nd} (Roberts et al., 2010; Piotrowski et al., 2012; Roberts et al., 2012; Tachikawa et al., 2013), although to date, there has not been a systematic comparison of ε_{Nd} in core-top unclean planktonic and seawater collected from the same sites. Recent work also indicates that in continental margin settings with relatively high concentrations of suspended particles, seawater ε_{Nd} may be modified by boundary exchange, compromising its utility as a watermass indicator (Lacan and Jeandel, 2005).

To evaluate potential issues with the ε_{Nd} proxy, we collected seawater and sediment samples along a depth transect (~380–3200 m) on the Demerara Rise, through Central Waters, AAIW, and NADW. We first assess the utility of unclean foraminifera ε_{Nd} as a reliable proxy for seawater ε_{Nd} by generating paired measurements of ε_{Nd} on unclean foraminifera from the tops of multi-cores, bottom water samples collected from the same multi-core sites, and water column samples collected offshore with hydrocasts. We then present three new deglacial ε_{Nd} records from modern AAIW depths on the Demerara Rise in the western tropical North Atlantic. We compare our new ε_{Nd} records with other published deepwater records to investigate the relationship between AAIW variability in the Atlantic with Atlantic deepwater variability and Pacific Ocean intermediate water variability. Finally, we discuss the climatic implications of our findings.

2. Materials and methods

2.1. Sediment cores and age models

We measured ε_{Nd} on unclean foraminifera from high-accumulation-rate sediment cores recovered from the Demerara Rise from AAIW depths (KNR197-3-25GGC, 7°42.27′N, 53°47.12′W, 671 mwd; KNR197-3-46CDH, 7°50.16′N, 53°39.80′W, 947 mwd; and KNR-197-3-9GGC, 7°55.80′N, 53°34.51′W, 1100 mwd) (Figs. 1 and 2). Low-salinity AAIW is evident between ~500 and 1100 m (Figs. 1B and 2), sandwiched in between higher salinity Atlantic Central Waters above and NADW below. Thus, our records come from (1) within the core of AAIW but near the transition to Atlantic Central Waters above, (2) within the core of AAIW (KNR197-3-25GGC) and (3) near the transition between AAIW and northern source waters below (KNR197-3-9GGC).

The chronology for KNR197-3-46CDH was constrained by 12 radiocarbon dates on planktonic foraminifera, which were converted to calendar age using the mean ocean reservoir (R) age (e.g. $\Delta R = 0$), and Calib6.0 using the Marine09 calibration curve (Table A.2) (Reimer et al., 2009). Three additional dates all measured on mixed layer planktonic foraminifera or mixed layer planktonic foraminifera combined with deeper dwellers were omitted from the age model (see Fig. A.1). At one of these depths (166.5 cm), we also measured the radiocarbon age of only deeper dwelling planktonic foraminifera, and this sample gave an age that is more consistent with the ages of sediment above and below this depth. At the other depth (200.5 cm), we measured the radiocarbon age of benthic foraminifera (*Uvigerina spp.*), which also gave an age that was consistent with our age model. The reason for the anomalously young ages is unclear, but may indicate burrowing of sediment with younger ages, and having more abundant mixed layer planktonic foraminifera. Note that our ε_{Nd} analyses were on deep-dwelling planktonic foraminifera (e.g., *G. menardii*, *P. Obliquiloculata* and *G. tumida*) rather than the mixed layer foraminifera (*G. ruber* and *G. sacculifer*) that gave anomalous ages. The chronologies for KNR-197-3-9GGC and KNR197-3-25GGC are constrained by 5 and 8 radiocarbon dates on planktonic foraminifera, respectively, converted to calendar age (Table A.3). No age reversals occur in these two cores. Note that KNR197-3-25GGC just reached LGM sediment, with a bottom age of ~19.4 kyr B.P. Average accumulation rates are ~19 cm/kyr for KNR197-3-46CDH and KNR197-3-25GGC, and ~11 cm/kyr for KNR197-3-9GGC.

2.2. Sample preparation

During expedition KNR197-3 of the *R/V Knorr* in 2010, seawater samples ranging from 50 to 4670 mwd were collected with Niskin bottles mounted onto a CTD-rosette (hydrocasts 3CTD and 68CTD) (Fig. 2). Bottom water samples were taken with Niskin bottles attached to the multi-coring system. Filtered samples were acidified at sea to pH <2 with ultrapure concentrated HCl and then stored in acid-washed 5-l polypropylene containers. Seawater samples were pre-concentrated using $Fe(OH)_3$-coprecipitation, and further purified through Eichrom 1-X8, TRU spec and LN spec resins. Nd purification followed the method established by our earlier work (Huang et al., 2012).

Approximately 2–3 mg of mixed thermocline- and deep-dwelling planktonic foraminifera (no *G. ruber* or *G. sacculifer*) were picked from the >63-μm size fraction of each sample. For

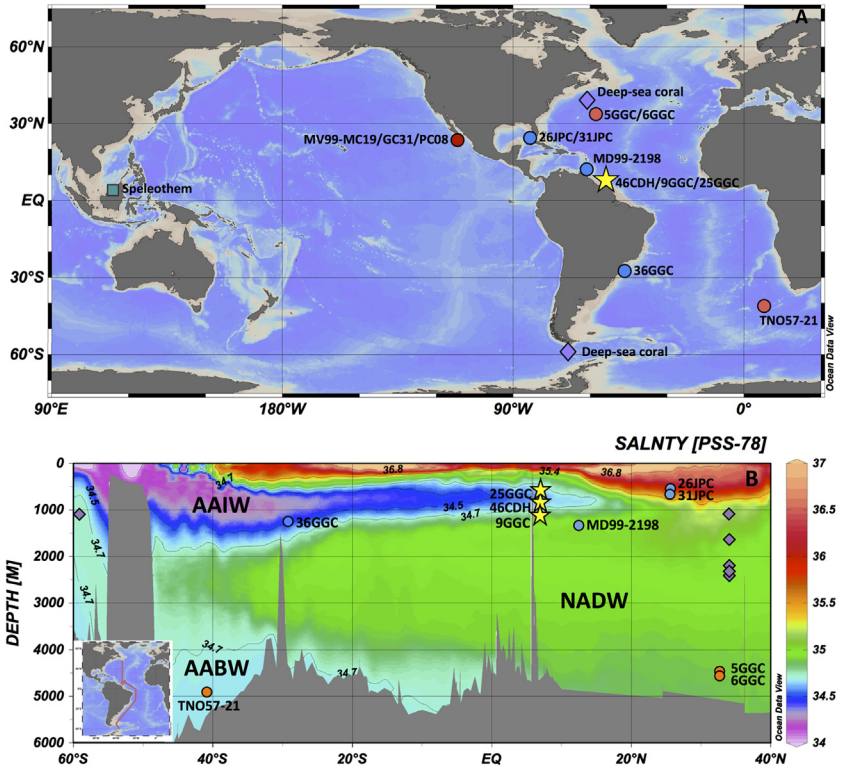

Fig. 1. (A) The locations of records discussed in text (see Table A.1): KNR197-3-46CDH, KNR197-3-9GGC and KNR197-3-25GGC (yellow stars, this study); ε_{Nd} records reconstructed from deep-sea corals, fish debris, unclean foraminifera and reductive leachates (purple diamonds, dark red circle, light red circles and blue circles, respectively) (van de Flierdt et al., 2006; Pahnke et al., 2008; Robinson and van de Flierdt, 2009; Basak et al., 2010; Roberts et al., 2010; Piotrowski et al., 2012); Borneo stalagmite $\delta^{18}O$ records (green square) (Partin et al., 2007). (B) Labeled sediment core sites plotted on the salinity section along the western Atlantic Ocean. AAIW: Antarctic Intermediate Water; AABW: Antarctic Bottom Water; NADW: North Atlantic Deep Water. Purple diamonds indicate the latitudes and water depths of deep-sea coral samples. Figures were made using Ocean Data View (http://odv.awi.de) (Schlitzer, 2000). (For interpretation of the references to color in this figure legend, the reader is referred to the web version of this article.)

some samples, ~5 mg of planktonic foraminifera were picked for duplicate measurements. Picked foraminiferal shells were gently crushed between glass slides under the microscope to ensure that all chambers were opened, and ultrasonicated five times for two minutes, three times with MilliQ-water, and two times with methanol. Samples were allowed to settle between ultrasonicating steps, before the rinse fluid was siphoned. Each sample was rinsed further with MilliQ-water until the solution was clear and free of clay. The cleaned samples were dissolved in weak acetic acid (Roberts et al., 2010). Bulk sediment leachates were prepared from <63-μm-size fraction following established procedures (Piotrowski et al., 2004; Gutjahr et al., 2007; Pahnke et al., 2008). Briefly, after leaching with 10 ml of buffered acetic acid for at least one day to remove the carbonate fraction, ~100 mg of sediment was leached for one hour with 10 ml of 0.02 M hydroxylamine hydrochloride (HH) in acetic acid to extract Fe–Mn fractions. The residue sediment was further leached with 1 M HH solution overnight to remove all remaining Fe–Mn oxides, and was completely digested in 4:1 hydrofluoric acid and perchloric acid. All the dissolved samples were passed through our two-step mini-columns (Eichrom TRU spec + Ln resin) to further purify Nd (Huang et al., 2012).

2.3. Nd isotope analysis

The Nd isotopic composition in seawater, bottom water, unclean foraminifera, sediment leachates, and detrital fractions were determined by Neptune MC-ICP-MS using a high-sensitivity desolvator (ARIDUS II, Cetac) at WHOI. The standard exponential law was used for correction of the instrumental mass discrimination with internal normalization to $^{146}Nd/^{144}Nd = 0.7219$. A 2.5 ng ml^{-1} JNdi-1 standard solution was used as a bracketing standard to monitor and correct for the instrumental mass fractionation. Another Nd standard solution, La Jolla, was also analyzed as a secondary reference to optimize instrumental conditions, and to further confirm data quality. Detailed information and quality assurance/control of the analytical technique can be found in our previous work (Huang et al., 2012). The $^{143}Nd/^{144}Nd$ ratios are reported as ε_{Nd}, that is, as deviations from the CHUR standard (CHUR = 0.512638; Jacobsen and Wasserburg, 1980), where

$$\varepsilon_{Nd} = \left[\frac{\left(\frac{^{143}Nd}{^{144}Nd}\right)_{Sample}}{\left(\frac{^{143}Nd}{^{144}Nd}\right)_{CHUR}} - 1 \right] \times 10\,000.$$

During the analytical course for seawater samples, the GEOTRACES intercalibration seawater standard, SAFE (3000 m), was also processed and analyzed using our method. The measured ε_{Nd} value for SAFE is -3.3 ± 0.3 (2SD, $n = 6$), consistent with the previously published result (-3.2 ± 0.5; van de Flierdt et al., 2012). The external reproducibility ($\pm 0.3\varepsilon$, 2SD) was assessed by our long-term runs of several international Nd isotopic standards, including JNdi-1, SAFE seawater, as well as Nod-P-1 Mn nodule (Huang et al., 2012).

3. Results and discussion

3.1. In situ multicore-top calibration

To systematically assess the utility of unclean foraminiferal ε_{Nd} as a reliable proxy for seawater ε_{Nd} in our study area, we conducted a series of ε_{Nd} measurements on multicore-top mixed planktonic foraminifera, ambient bottom water collected with the

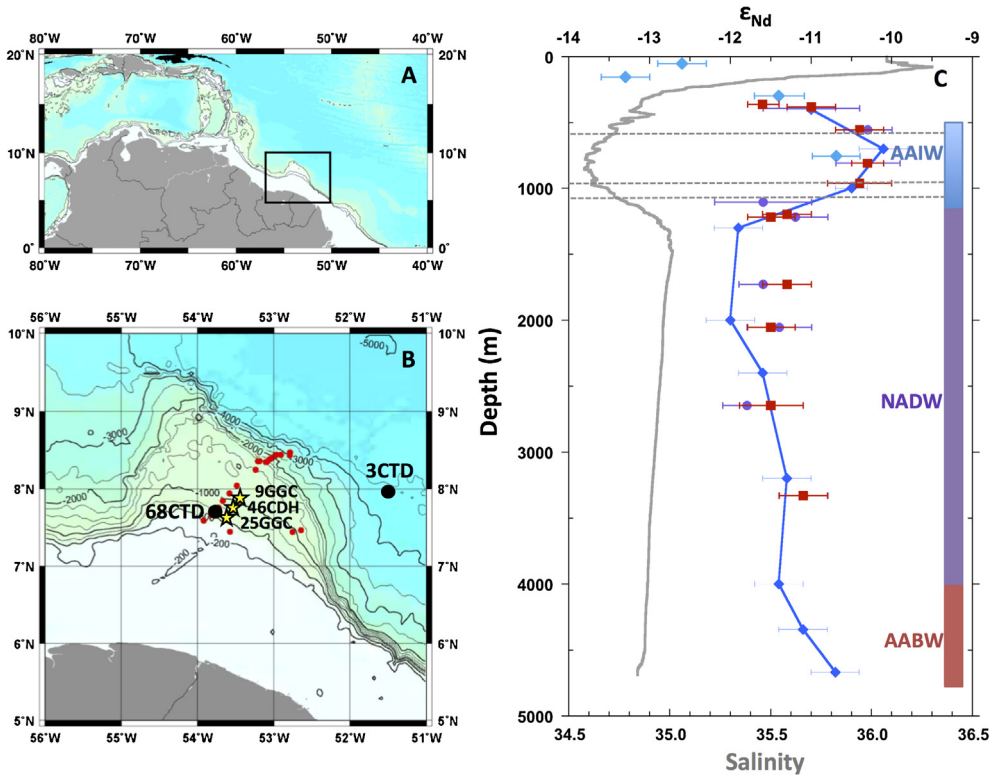

Fig. 2. Sample locations and comparison of seawater ε_{Nd} and unclean foraminifera ε_{Nd} of study sites. (A) Map of Demerara Rise study area. (B) The locations of seawater (black circles), multicores (red circles) and sediment cores (KNR-197-3-46CDH, 947 mwd; KNR197-3-9GGC, 1100 mwd; KNR197-3-25GGC, 671 mwd; yellow stars). (C) Comparison of ε_{Nd} values of seawater (blue diamonds), bottom water (purple circles) and multicore-top unclean foraminifera (red squares). The gray line shows the salinity profile in our study area. Horizontal gray dashed lines indicate the water depths for the three ε_{Nd} records presented in this study. The color bars on the right indicate the approximate depths of AAIW, NADW and AABW in our study area. (For interpretation of the references to color in this figure legend, the reader is referred to the web version of this article.)

multi-coring system, and offshore seawater collected on CTD hydrocasts (Fig. 2C, Tables A.4–A.6). The ε_{Nd} values of the offshore seawater range from −10 to −12 at depths of 500–4670 m, and the vertical profile of seawater ε_{Nd} (including bottom water) mimics that of salinity ($r = 0.89$; $p = 0.001$) and the main water masses at our study site, confirming that seawater Nd isotopes is a useful water mass tracer in this region. At depths shallower than 150 m (68CTD), seawater ε_{Nd} values are much less radiogenic (∼−13), most likely reflecting either an atmospheric input or ε_{Nd} signature advected from the east in the North Equatorial Current, as suggested by Piepgras and Wasserburg (1987). Similar values in water column samples and bottom waters, and their correlations with salinity, suggest that the seawater ε_{Nd} is not influenced locally by boundary exchange. This inference is further supported by a ∼1 difference between ε_{Nd} values of bottom water ($\varepsilon_{Nd} = -10.3$) and detrital sediment ($\varepsilon_{Nd} = -11.2$) from the shallowest core depths (10.5 cm, 3.7 kyr B.P.) of core KNR197-3-46CDH. Similar ε_{Nd} values in unclean foraminifera and seawater across our depth transect demonstrate, unequivocally, that unclean foraminifera record the ε_{Nd} of seawater with the fidelity to distinguish between the different water masses in our study area (Fig. 2 and Fig. 3).

3.2. Down-core Demerara Rise ε_{Nd} of unclean foraminifera

Our new ε_{Nd} records of unclean foraminifera (Fig. 4, Tables A.7–A.9) reveal that LGM seawater ε_{Nd} values were either slightly more radiogenic than (e.g. KNR197-3-46CDH; $\varepsilon_{Nd} = \sim -9.8 \pm 0.4$, average ε_{Nd} value between 19 and 23 kyr B.P. ±1 SD) or comparable to (KNR197-3-25GGC and KNR197-3-9GGC) the modern value of −10.6. Two unradiogenic ε_{Nd} excursions coincident with HS1 and the YD were superimposed on these small

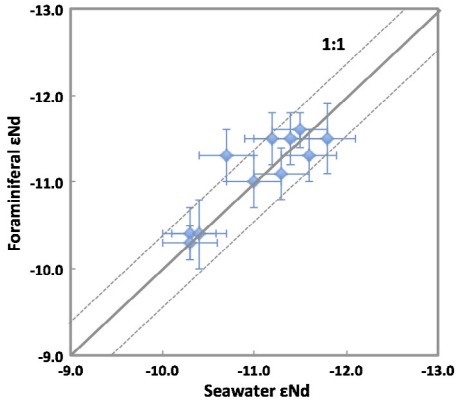

Fig. 3. Unclean foraminiferal ε_{Nd} versus seawater ε_{Nd} collected from the Demerara Rise, western tropical North Atlantic. The 1:1 line (gray line) is plotted for comparison and the gray dashed lines indicate the external reproducibility (±0.3ε, 2SD) of our analytical technique. Error bars for all reported data represent external reproducibility. When the internal error is larger than the external reproducibility, a combined error, $\sqrt{(\text{internal error}^2 + \text{external error}^2)}$, is used.

LGM-to-Holocene changes at all three water depths. Before discussing insights on AAIW variability provided by these results, we discuss other potential influences on these records.

3.3. Effect of boundary exchange on unclean foraminiferal ε_{Nd}

Recent studies suggest that boundary exchange, involving the exchange reaction with continental sediments, may contribute to non-conservative behavior of Nd in the modern oceans (Lacan and Jeandel, 2005; Wilson et al., 2012). In order to systematically eval-

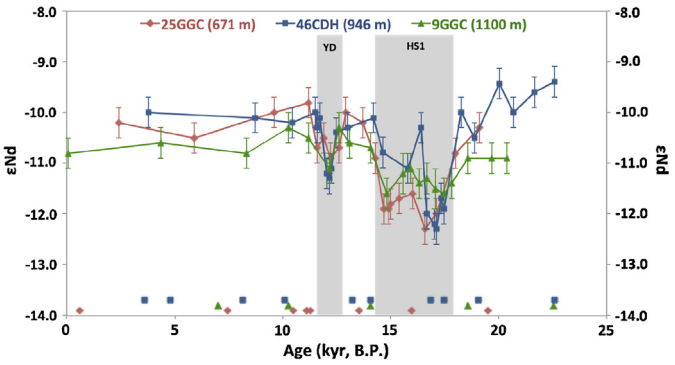

Fig. 4. Comparison of reconstructed seawater ε_{Nd} records for KNR197-3-25GGC (red diamonds), KNR197-3-46CDH (blue squares) and KNR197-3-9GGC (green triangles). Age control points are indicated for using the same symbols. Gray shadings mark the deglacial North Atlantic cold events (YD and HS1). (For interpretation of the references to color in this figure legend, the reader is referred to the web version of this article.)

uate the potential effect of boundary exchange on our down-core unclean foraminifera ε_{Nd} record, Nd isotope measurements were made on the detrital fraction of a subset of samples from core KR197-3-46CDH. The unradiogenic ε_{Nd} of the detrital sediment (Fig. A.2 and Table A.7), ranging from −11 to −13, supports a dominant sediment source from mixing of Amazon River sediment ($\varepsilon_{Nd} = \sim -9.2$; Goldstein et al., 1984), Orinoco River sediment ($\varepsilon_{Nd} = \sim -13$; White et al., 1985), and presumably sediments supplied by Essequibo River, a small local river. The correlation ($r = 0.34$, $p = 0.26$) between unclean foraminifera ε_{Nd} and detrital sediment ε_{Nd} (Fig. A.2) is not significant. We presume, therefore, that our unclean foraminifera ε_{Nd} record is not influenced by exchange with contemporary detrital material.

3.4. Down-core sediment leachate ε_{Nd} record

Previous studies have used records of authigenic ε_{Nd} from sediment leachates to reconstruct deglacial AAIW variability in the Atlantic Ocean (Pahnke et al., 2008; Xie et al., 2012). However, recent work demonstrates that reconstructions of ε_{Nd} variability using the authigenic leachate fraction may be significantly modified by preferential leaching of volcanic material, and often does not record the seawater value (Roberts et al., 2010; Elmore et al., 2011; Wilson et al., 2013; Kraft et al., 2013). We also made authigenic ε_{Nd} measurements on leachates from bulk sediments (<63-μm-size fraction; Fig. A.3 and Table A.10) in a subset of samples from KNR197-3-46CDH to evaluate the fidelity of the leachate records in our study site and to compare with existing leachate records from the intermediate-depth Atlantic (Fig. A.4). Several lines of evidence suggest that ε_{Nd} measured on sediment leachates do not represent seawater values at our study site. First, the ε_{Nd} value of the late Holocene (~3.7 kyr B.P.) sediment leachates ($\varepsilon_{Nd} = \sim -9$) deviates significantly from the modern seawater ε_{Nd} value ($\varepsilon_{Nd} = -10.6$) at around 1000 m. Second, the correlation between unclean foraminifera ε_{Nd} and sediment leachate ε_{Nd} is not significant ($r = 0.31$, $p = 0.31$; Fig. A.3). Although two unradiogenic ε_{Nd} excursions also occur approximately coincident with HS1 and YD in the sediment leachate ε_{Nd} records from the Demerara Rise and Florida Straits (Xie et al., 2012), the timing and duration of these sediment leachate ε_{Nd} events differ from the events as recorded in Demerara Rise unclean foraminifera (Fig. A4). Nd isotope records of unclean foraminifera from the Florida Margin would be useful for assessing whether intermediate depth (550–750 m) seawater ε_{Nd} variations at these sites are in fact coherent with those measured at the Demerara Rise.

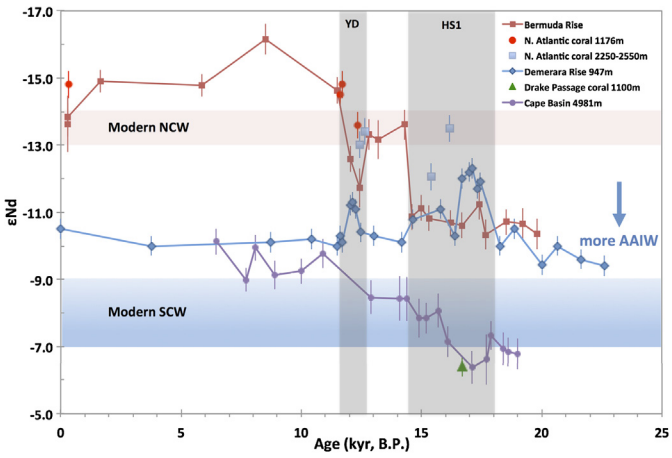

Fig. 5. Comparison between unclean foraminifera ε_{Nd} from KNR197-3-46CDH and other unclean foraminifera/deep-sea coral ε_{Nd} records from mid-depth and deep Atlantic Ocean (see Table A.1). Blue and red shaded areas represent the modern seawater ε_{Nd} values for Southern Component Water (SCW) and Northern Component Water (NCW), respectively. Gray shaded areas highlight the deglacial North Atlantic cold events (YD and HS1). (For interpretation of the references to color in this figure legend, the reader is referred to the web version of this article.)

3.5. Changes in endmember ε_{Nd} values of northern and southern component waters

Previous studies suggest that the endmember ε_{Nd} compositions of northern-sourced waters in the North Atlantic remain constant on glacial–interglacial timescales through the Pleistocene (van de Flierdt et al., 2006; Foster et al., 2007), although more data are needed to claim this with confidence. The Southern Ocean ε_{Nd} value, which reflects the balance between input of North Atlantic and Pacific waters, seems to have become more Pacific-like (more radiogenic) during the LGM, suggesting the export of northern source water to the Southern Ocean decreased (Fig. 5; Piotrowski et al., 2012), and such a decrease may have contributed to the more radiogenic values during the LGM than the Holocene at KNR197-3-46CDH, within the core of AAIW (~950 mwd). One LGM data point from KNR197-3-25GGC, also within the core of AAIW (~650 m), similarly suggests more radiogenic glacial values. There was no perceptible LGM–Holocene change at KNR197-3-9GGC, which is on the transition between AAIW and northern source water.

Coral ε_{Nd} data from the intermediate-depth North Atlantic (~39°N) hint at more radiogenic values during the peak of the YD compared to the end of the YD (Fig. 5) (van de Flierdt et al., 2006), suggesting that the unradiogenic values we document during the peak of the YD in the intermediate depth tropical North Atlantic are not due to a change in the northern endmember value. The Southern Ocean ε_{Nd} value, which reflects the balance between input of North Atlantic and Pacific waters, is also likely to have become more radiogenic due to reduced export of northern source water to the Southern Ocean, especially during events of reduced AMOC (e.g., HS1 and YD). Indeed, the only direct evidence to constrain the endmember ε_{Nd} value of the intermediate-depth Southern Ocean is from fossil deep-sea corals (~1100 m) in the Drake Passage (the source region of AAIW), which suggests that seawater was significantly more radiogenic during HS1 (-6.4 ± 0.4; Robinson and van de Flierdt, 2009) than the modern day ($\varepsilon_{Nd} = -9$; Piepgras and Wasserburg, 1982; Stichel et al., 2012). Recently published ε_{Nd} data of unclean planktonic foraminifera from the deep South Atlantic (Fig. 5) (Piotrowski et al., 2012) also suggest more radiogenic Southern Ocean values during North Atlantic cold events. Therefore, the less radiogenic values we observe during North Atlantic cold events do not appear

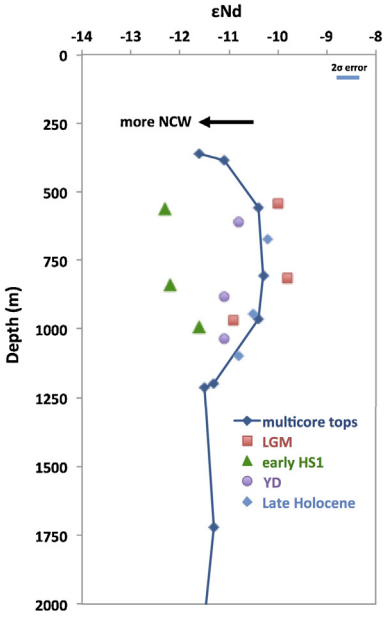

Fig. 6. Depth transect of reconstructed seawater ε_{Nd} during the LGM (red squares), early HS1 (green triangles), YD (purple circles) and Late Holocene (light blue diamonds). Multicore-top ε_{Nd} values (blue diamonds with line) are shown for comparison. Note that water depths for the LGM, early HS1 and YD are corrected for sea-level changes based on Clark et al. (2009). (For interpretation of the references to color in this figure legend, the reader is referred to the web version of this article.)

to be due to a change in the southern source endmember value. Instead, the more radiogenic Southern Ocean values suggest that the Demerara Rise record may underestimate water mass variability. Clearly, reliable ε_{Nd} records from the water mass source regions are needed to better constrain possible ε_{Nd} endmember changes. Nevertheless, based on the available data, the millennial excursions at our core site towards less radiogenic values are unlikely to result solely from endmember changes.

3.6. Western Atlantic AAIW variability inferred from ε_{Nd}

To facilitate visualization of changes in ε_{Nd} with depth we compare ε_{Nd} values during the LGM (23–19 kyr B.P., only one point for KNR197-3-25GGC), the peak excursion in early HS1 (17–16.7 kyr P.B.), and the peak YD excursion (~12.2 kyr B.P.) to core-top values (Fig. 6). As discussed above, a more radiogenic southern endmember ε_{Nd} value may have resulted in more radiogenic LGM ε_{Nd} values within the core of AAIW at the Demerara Rise (at our two shallowest sites). However, because more radiogenic values are only found in the two shallowest cores, they may indicate a greater fraction of AAIW in its core (an intensification of AAIW) during the LGM.

The most likely explanation for the less radiogenic ε_{Nd} values during HS1 and the YD is an increased fraction of northern source water relative to AAIW. During early HS1, ε_{Nd} values suggest that northern source water were the dominant watermass in the tropical North Atlantic at modern AAIW depths, whereas during the YD, these waters seem to have still contained a contribution of AAIW. Our results provide the strongest evidence yet that AAIW flow into the North Atlantic did not increase as previously suggested (e.g. Pahnke et al., 2008; Pena et al., 2013), but instead, was reduced during North Atlantic cold events (e.g. Came et al., 2008; Xie et al., 2012). Our study does not address whether the shallower return flow (the "warm water" pathway; Gordon et al., 1992) into the North Atlantic also decreased during these intervals. However, modeling studies suggest that the surface and thermocline return flow is weaker during times of reduced overturning, leading to a

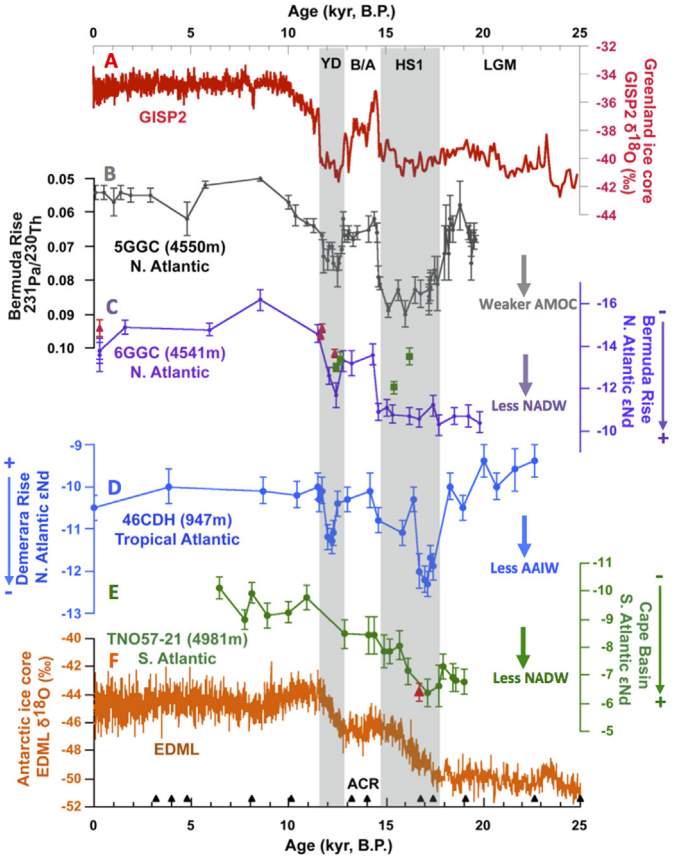

Fig. 7. Comparison of unclean foraminifera ε_{Nd} record from KNR197-3-46CDH and other climate records. (A) $\delta^{18}O$ record of ice from Greenland Ice Sheet Project (GISP2; Grootes and Stuvier, 1997); (B) OCE326-5GGC $^{231}Pa/^{230}Th$ ratios (deep North Atlantic, 4550 m; McManus et al., 2004); (C) OCE326-6GGC unclean foraminifera ε_{Nd} (deep North Atlantic, 4541 m; Roberts et al., 2010). Deep-sea coral ε_{Nd} from New England Seamounts chain (red triangles: 1176 m water depth; green squares: 2250–2550 m water depth; van de Flierdt et al., 2006); (D) KNR197-3-46CDH unclean foraminifera ε_{Nd} (blue line and circles, western tropical North Atlantic, 947 m). Note that the Demerara Rise ε_{Nd} record is plotted on a reversed axis; (E) TNO57-21 unclean foraminifera ε_{Nd} (green circles, deep South Atlantic, 4981 m; Piotrowski et al., 2012). A deep-sea coral ε_{Nd} from Drake Passage during Heinrich Stadial 1 is also shown (Robinson and van de Flierdt, 2009); (F) $\delta^{18}O$ record of ice from EPICA Dronning Maudland (EDML; Barbante et al., 2006). Age control points (black triangles) are indicated for KNR197-3-46CDH. The Last Glacial Maximum (LGM), Heinrich Stadial 1 (HS1), Bølling–Allerød (B/A), Younger Dryas (YD) and Antarctic Cold Reversal (ACR) are indicated. (For interpretation of the references to color in this figure legend, the reader is referred to the web version of this article.)

warming of the south Atlantic thermocline (e.g., Dahl et al., 2005). As warming extends to AAIW depths, we infer that the AAIW return flow is also reduced in these experiments, consistent with our interpretation.

3.7. Deglacial water mass and AMOC variability

Comparison of our new ε_{Nd} records to the other Atlantic records of ε_{Nd} measured on unclean foraminifera (Fig. 7; we show only KNR197-3-46CDH for clarity) reveals a nearly anti-phase behavior between our shallow records and deeper records on millennial time scales. For example, during early HS1, the AAIW decrease we infer at the Demerara Rise is mirrored by more radiogenic values in the deep Cape Basin, implying less NADW export to the South Atlantic. The absence of a related feature at the Bermuda Rise seems to imply little water mass variability in the deep North Atlantic at this time. As at our two shallower Demerara Rise sites, the deepwater response in the deep Cape Basin was muted late in the Heinrich event. The ε_{Nd} values during the Bølling–Allerød

imply a deepwater mass geometry similar to the modern one. A convergence between intermediate-depth tropical North Atlantic and deep North Atlantic values during the YD implies that reduced AAIW contribution to the upper tropical North Atlantic was associated with reduced export of NADW to depth.

Changes in deepwater geometry as inferred from ε_{Nd}, bear a strong resemblance to AMOC variations inferred from sedimentary $^{231}Pa/^{230}Th$ ratios (e.g. McManus et al., 2004), suggesting that at least in a broad sense, millennial changes in deepwater geometry are coupled to changes in AMOC intensity. However, in contrast with sedimentary $^{231}Pa/^{230}Th$ records (McManus et al., 2004; Gherardi et al., 2009) (Fig. 7) and with AAIW previously inferred from leachate ε_{Nd} (Xie et al., 2012) (Fig. A.4), all three Demerara Rise suggest two stages of reduced AAIW influence during HS1 – an early stage (from ~18 to 16 kyr B.P.) in which ε_{Nd} values of all three records approach modern North Atlantic endmember values, and a later stage (15.5–14.7 kyr B.P.), when intermediate values suggest a smaller reduction in the fraction of AAIW (Fig. 4). These episodes are separated by a return to the modern ε_{Nd} value in one core (KNR197-3-46CDH), but the return is more modest in the other two cores. Additional data are needed to confirm these differences.

In our two highest deposition rate (shallowest) cores, both within AAIW, the early HS1 ε_{Nd} excursion is larger than the later one. Given additional evidence from the deep Cape Basin, which shows a much more significant ε_{Nd} excursion during early than late HS1 (Fig. 7), we speculate that the AMOC was weaker during early than late HS1. If that is the case, a weaker AMOC during early HS1 may explain why tropical atmospheric circulation and hydrologic change, as reflected in the oxygen isotope composition of tropical speleothems from the deep tropics (Fig. 7F), was more anomalous early in the Heinrich stadial (e.g., Partin et al., 2007). Combined with modeling studies evaluating the global climate response to events of reduced AMOC (e.g., Vellinga and Wood, 2002; Lewis et al., 2010), our data suggest that these pronounced early Heinrich climate anomalies were caused by a dramatically curtailed AMOC, which partially recovered later in the Heinrich stadial. More broadly, our evidence of two distinct phases within HS1 of reduced AAIW return flow, and by inference, of AMOC reduction, may help explain widespread evidence of differing hydrologic conditions during these two intervals (Broecker and Putnam, 2012). Furthermore, if a weak AMOC is a key element in the deglacial atmospheric CO_2 rise, because, for example, it results in reduced Antarctic stratification (e.g., Sigman et al., 2007; Anderson et al., 2009; Toggweiler and Lee, 2010), our evidence of weaker AMOC early in HS1 also explains why atmospheric CO_2 rose more rapidly during early than late HS1 (e.g. Monnin et al., 2001).

3.8. Deglacial variability of AAIW in the Pacific and Atlantic Ocean

Notably, the HS1 and YD negative ε_{Nd} excursions we document at AAIW depths in the tropical North Atlantic coincide with excursions to positive ε_{Nd} values in a sediment core from 681 m water depth off Baja California, northeast Pacific (Fig. 8D). The Pacific data may indicate a greater contribution of modified AAIW relative to North Pacific Intermediate Water (NPIW) during early HS1 and the YD (Basak et al., 2010). In the Pacific, AAIW subducts northward from its surface source region (mainly in the southeast Pacific, off southern Chile) along an isopycnal surface between 600 and 1300 m, and then follows the wind-driven subtropical gyre surface water circulation (McCartney, 1982; Tomczak and Godfrey, 1994; Reid, 1997; Talley, 1999; Sloyan and Rintoul, 2001). The northward transport of AAIW in the southeast Pacific appears to be balanced by a southward flow along the western boundary of the basin (Sloyan and Rintoul, 2001). Several possible mechanisms may explain the apparent teleconnection between intermediate water circulation in these two ocean basins: [1] during millennial events of AMOC reduction, NPIW may have deepened (Okazaki et al., 2010), allowing AAIW to extend farther north in the Pacific Ocean compared to the Atlantic Ocean; [2] stronger westerlies in the South Pacific sector during North Atlantic cooling (Lee et al., 2011) may have promoted AAIW formation in the Pacific Ocean; [3] AAIW that was previously drawn northward into the North Atlantic to replace exported deep water more readily flowed into the interior of the Pacific. This latter mechanism would not require a change in AAIW production rate, only a rerouting from the Atlantic to the Pacific in response to reduced demand to replace NADW that was exported at depth. Although the potential mechanisms need to be explored further, together with evidence linking two phases of reduced AAIW flow into the North Atlantic during HS1 with two phases in the hydrologic cycle, our evidence of antiphased ε_{Nd} behavior between intermediate depths of the North Atlantic and Pacific (implying an oceanographic response in the high latitude formation region of NPIW and/or AAIW) underscores the global reach of North Atlantic abrupt climate change.

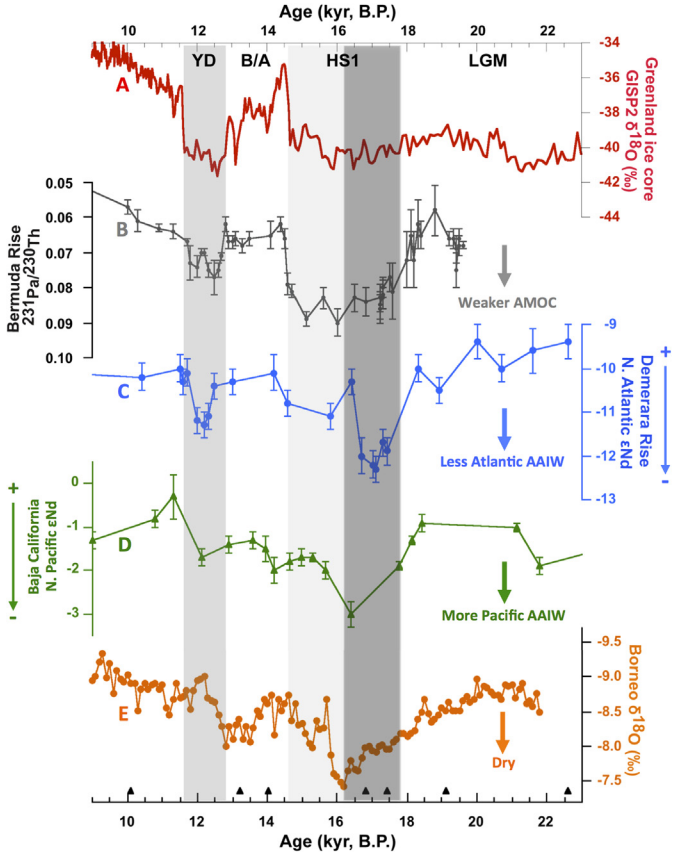

Fig. 8. Multi-proxy records during the LGM and last deglaciation (9–23 kyr B.P.) in the Atlantic and Pacific Ocean. (A) $\delta^{18}O$ record of GISP2 (Grootes and Stuvier, 1997); (B) Sedimentary $^{231}Pa/^{230}Th$ ratios of OCE326-5GGC (McManus et al., 2004); (C) Unclean foraminifera ε_{Nd} of KNR197-3-46CDH; (D) Fish debris ε_{Nd} record of MV99-MC19/GC31/PC08 (Basak et al., 2010); (E) $\delta^{18}O$ record of Borneo stalagmite (Partin et al., 2007). Age control points (black triangles) are indicated for KNR197-3-46CDH. The LGM, HS1, B/A and YD are indicated. The two-phase HS1 is also indicated based on Broecker and Putnam (2012).

4. Conclusions

Depth transects of ε_{Nd} measured on seawater and unclean foraminifera from the Demerara Rise in the western tropical North Atlantic confirm the quasi-conservative properties of seawater ε_{Nd}, its utility as a water mass tracer, and the ability of unclean foraminifera to faithfully record bottom water ε_{Nd} values in their

authigenic coatings. We present the first foraminifera-based reconstructions of seawater ε_{Nd} from sediment cores from within AAIW depths in the western tropical North Atlantic. Foraminiferal ε_{Nd} variations are not significantly correlated to variations in ε_{Nd} of sediment leachates from the same core, suggesting that in this region, Nd isotope variability of sediment leachates does not accurately reflect deepwater variability. Our new unclean foraminifera-based ε_{Nd} records suggest that AAIW still reached the Demerara Rise during the LGM, but reveal a pronounced decrease in the fraction of AAIW during North Atlantic deglacial cold episodes HS1 and YD, consistent with hypothesized AMOC reduction during these events. Our data reveal two phases of reduced AAIW fraction within HS1, with the greatest reduction early in HS1, the period marked by massive iceberg discharge. If the AAIW fraction reflects the AMOC, as we hypothesize, then this finding may explain why, in many regions, there are distinct climate anomalies in early and late HS1, and why atmospheric CO_2 rose faster during early than late HS1. In contrast to our ε_{Nd} record, an intermediate-depth record from the northeast Pacific suggests more radiogenic values during the same millennial events, potentially indicating that the flow of AAIW into the Atlantic and Pacific seesaws on millennial time scales.

Acknowledgements

We thank the captain, crew and scientific team of the cruise KNR197-3 of R/V Knorr for a successful cruise. Special thanks to K. Rose, M. Jeglinski, E. Bonk and G. Toltin for lab assistance, J. Blusztajn for technical support and maintenance of Neptune MC-ICP-MS, D. Thornalley for helpful discussions, and K. Pahnke for providing the GEOTRACES intercalibration seawater sample (SAFE, 3000 m). We are very grateful for the comments of two anonymous reviewers. This work was supported by US NSF grants and a Lawrence J. Pratt and Melinda M. Hall Endowed Fund for Interdisciplinary Research Award to D.W.O. and W.B.C. and by a Taiwan NSC Postdoctoral Fellowship (NSC98-2917-I-564-132) to K.F.H.

Appendix A. Supplementary material

Supplementary material related to this article can be found online at http://dx.doi.org/10.1016/j.epsl.2013.12.037.

References

Anderson, R.F., Ali, S., Bradtmiller, I., Nielsen, S.H.H., Fleisher, M.Q., Anderson, B.E., Burckle, L.H., 2009. Wind-driven upwelling in the Southern Ocean and the deglacial rise in atmospheric CO_2. Science 323, 1443–1448.

Arsouze, T., Dutay, J.C., Lacan, F., Jeandel, C., 2009. Reconstructing the Nd oceanic cycle using a coupled dynamical–biogeochemical model. Biogeosciences 6, 2829–2846.

Barbante, C., et al., 2006. One-to-one coupling of glacial climate variability in Greenland and Antarctica. Nature 444, 195–198.

Basak, C., Martin, E.E., Horikawa, K., Marchitto, T.M., 2010. Southern Ocean source of ^{14}C-depleted carbon in the North Pacific Ocean during the last deglaciation. Nat. Geosci. 3, 770–773.

Boyle, E.A., Keigwin, L.D., 1987. North-Atlantic thermohaline circulation during the past 20,000 years linked to high-latitude surface temperature. Nature 330, 35–40.

Broecker, W.S., Putnam, A.E., 2012. How did the hydrologic cycle response to the two-phase mystery interval? Quat. Sci. Rev. 57, 17–25.

Came, R.E., Oppo, D.W., Curry, W.B., Lynch-Stieglitz, J., 2008. Deglacial variability in the surface return flow of the Atlantic meridional overturning circulation. Paleoceanography 23, PA1217. http://dx.doi.org/10.1029/2007PA001450.

Chase, Z., Anderson, R.F., Fleisher, M.Q., Kubik, P.W., 2002. The influence of particle composition and particle flux on scavenging of Th, Pa and Be in the ocean. Earth Planet. Sci. Lett. 204, 215–229.

Clark, P.U., Dyke, A.S., Shakun, J.D., Carlson, A.E., Clark, J., Wohlfarth, B., Mitrovica, J.X., Hostetler, S.W., McCabe, A.M., 2009. The last glacial maximum. Science 325, 710–714.

Curry, W.B., Duplessy, J.C., Labeyrie, L.D., Shackleton, N.J., 1988. Changes in the distribution of $\delta^{13}C$ of deep water ΣCO_2 between the last deglaciation and the Holocene. Paleoceanography 3, 317–341.

Curry, W.B., Oppo, D.W., 2005. Glacial water mass geometry and the distribution of $\delta^{13}C$ of ΣCO_2 in the western Atlantic Ocean. Paleoceanography 20, PA017. http://dx.doi.org/10.1029/2004PA001021.

Dahl, K.A., Broccoli, A.J., Stouffer, R.J., 2005. Assessing the role of North Atlantic freshwater forcing in millennial scale climate variability: a tropical Atlantic perspective. Clim. Dyn. 24, 325–346.

Duplessy, J.C., Shackleton, N.J., Fairbank, R.G., Labeyrie, L., Oppo, D.W., Kallel, N., 1988. Deepwater source variations during the last climatic cycle and their impact on the global deepwater circulation. Paleoceanography 3, 343–360.

Elmore, A.C., Piotrowski, A.M., Wright, J.D., Scrivner, A.E., 2011. Testing the extraction of past seawater Nd isotopic composition from North Atlantic deep sea sediments and foraminifera. Geochem. Geophys. Geosyst. 12, Q09008. http://dx.doi.org/10.1029/2011GC003741.

Foster, G.L.D., Vance, D., Prytulak, J., 2007. No change in the neodymium isotope composition of deep water exported from the North Atlantic on glacial–interglacial time scales. Geology 35, 37–40.

Gherardi, J.M., Labeyrie, L., Nave, S., Francois, R., McManus, J.F., Cortijo, E., 2009. Glacial–interglacial circulation changes inferred from $^{231}Pa/^{230}Th$ sedimentary record in the North Atlantic region. Paleoceanography 24. http://dx.doi.org/10.1029/2008PA001696.

Goldstein, S.L., Hemming, S.R., 2003. Long-lived isotopic tracers in oceanography, paleoceanography, and ice-sheet dynamics. In: Treatise on Geochemistry. Elsevier, New York, pp. 453–489.

Goldstein, S.L., O'Nions, R.K., Hamilton, P.J., 1984. A Sm–Nd isotopic study of atmospheric dusts and particulates from major river systems. Earth Planet. Sci. Lett. 70, 221–236.

Gordon, A.L., Weiss, R.F., Smethie Jr., W.M., Warner, M.J., 1992. Thermocline and intermediate water communication between the South Atlantic and Indian Oceans. J. Geophys. Res. 97, 7223–7240.

Grootes, P., Stuvier, M., 1997. Oxygen 18/16 variability in Greenland snow and ice with 10^{-3} to 10^{-5} year resolution. J. Geophys. Res. 102, 26455–26470.

Gutjahr, M., Frank, M., Stirling, C.H., Klemm, V., van de Flierdt, T., Halliday, A.N., 2007. Reliable extraction of a deepwater trace metal isotope signal from Fe–Mn oxyhydroxide coatings of marine sediments. Chem. Geol. 242, 351–370.

Huang, K.-F., Blusztajn, J., Oppo, D.W., Curry, W.B., Peucker-Ehrenbrink, B., 2012. High-precision and accurate determination of neodymium isotopic compositions at nanogram levels in natural materials by MC-ICP-MS. J. Anal. At. Spectrom. 27, 1560–1567.

Jacobsen, S.B., Wasserburg, G.J., 1980. Sm–Nd isotopic evolution of chondrites. Earth Planet. Sci. Lett. 50, 139–155.

Jeandel, C., 1993. Concentration and isotopic composition of Nd in the South Atlantic Ocean. Earth Planet. Sci. Lett. 117, 581–591.

Keigwin, L.D., Lehman, S.J., 1994. Deep circulation change linked to Heinrich event 1 and Younger Dryas in a middepth North Atlantic core. Paleoceanography 9, 185–194.

Kraft, S., Frank, M., Hathorne, E.C., Weldeab, S., 2013. Assessment of seawater Nd isotope signatures extracted from foraminiferal shells and authigenic phases of Gulf of Guinea sediments. Geochim. Cosmochim. Acta 121, 414–435.

Kroopnick, P., 1980. The distribution of ^{13}C in the Atlantic Ocean. Earth Planet. Sci. Lett. 49, 469–484.

Lacan, F., Jeandel, C., 2005. Neodymium isotopes as a new tool for quantifying exchange fluxes at the continental–ocean interface. Earth Planet. Sci. Lett. 232, 245–257.

Lee, S.-Y., Chiang, J.C.H., Matsumoto, K., Tokos, K.S., 2011. Southern Ocean wind response to North Atlantic cooling and the rise in atmospheric CO_2: Modeling perspective and paleoceanographic implications. Paleoceanography 26, PA1214. http://dx.doi.org/10.1029/2010PA002004.

Lewis, S.C., LeGrande, A.N., Kelley, M., Schmidt, G.A., 2010. Water vapor source impacts on oxygen isotope variability in tropical precipitation during Heinrich events. Clim. Past 6, 325–343.

Lynch-Stiegkitz, J., et al., 2007. Atlantic meridional overturning circulation during the last glacial maximum. Science 316, 66–69.

Marchitto, T.M., Broecker, W.S., 2006. Deep water mass geometry in the glacial Atlantic Ocean: A review of constraints from the paleonutrient proxy Cd/Ca. Geochem. Geophys. Geosyst. 7, Q120003. http://dx.doi.org/10.1029/2006GC001323.

McCartney, M.S., 1982. The subtropical circulation of Mode Waters. J. Mar. Res. 40 (Suppl.), 427–464.

McManus, J.F., Francois, R., Gherardi, J.M., Keigwin, L.D., Brown-Leger, S., 2004. Collapse and rapid resumption of Atlantic meridional circulation linked to deglacial climate changes. Nature 428, 834–837.

Mix, A.C., Fairbanks, R.G., 1985. North Atlantic surface-ocean control of Pleistocene deep-ocean circulation. Earth Planet. Sci. Lett. 73, 231–243.

Monnin, E., et al., 2001. Atmospheric CO_2 concentrations over the last glacial termination. Science 291, 112–114.

Okazaki, Y., et al., 2010. Deepwater formation in the North Pacific during the last glacial termination. Science 329, 200–204.

Oppo, D.W., Curry, W.B., 2012. Deep Atlantic circulation during the Last Glacial Maximum and deglaciation. Nat. Educ. Knowl. 3, 1.

Pahnke, K., Goldstein, S.L., Hemming, S.R., 2008. Abrupt changes in Antarctic intermediate water circulation over the past 25,000 years. Nat. Geosci. 1, 870–874.

Palter, J.B., Lozier, M.S., 2008. On the source of Gulf Stream nutrients. J. Geophys. Res. 113, C06018. http://dx.doi.org/10.1029/2007JC004611.

Partin, J.W., Cobb, K.M., Adkins, J.F., Clark, B., Fernandez, D.P., 2007. Millennial-scale trends in west Pacific warm pool hydrology since the Last Glacial Maximum. Nature 449, 452–455.

Pena, L.D., Goldstein, S.L., Hemming, S.R., Jones, K.M., Calvo, E., Pelejero, C., Cacho, I., 2013. Rapid changes in meridional advection of Southern Ocean intermediate waters to the tropical Pacific during the last 30 kyr. Earth Planet. Sci. Lett. 368, 20–32.

Piepgras, D.J., Wasserburg, G.J., 1982. Isotopic composition of neodymium in waters from the Drake Passage. Science 217, 207–214.

Piepgras, D.J., Wasserburg, G.J., 1987. Rare earth element transport in the western North Atlantic inferred from Nd isotopic compositions. Geochim. Cosmochim. Acta 51, 1257–1271.

Piotrowski, A.M., Galy, A., Nicholl, J.A.L., Roberts, N., Wilson, D.J., Clegg, J.A., Yu, J., 2012. Reconstructing deglacial North and South Atlantic deep water sourcing using foraminiferal Nd isotopes. Earth Planet. Sci. Lett. 357–358, 289–297.

Piotrowski, A.M., Goldstein, S.L., Hemming, S.R., Fairbanks, R.G., 2004. Intensification and variability of ocean thermohaline circulation through the last deglaciation. Earth Planet. Sci. Lett. 225, 205–220.

Reid, J.L., 1997. On the total geostrophic circulation of the Pacific Ocean: Flow patterns, tracers and transports. Prog. Oceanogr. 39, 263–352.

Reimer, et al., 2009. IntCal09 and Marine09 radiocarbon age calibration curves, 0–50,000 years cal BP. Radiocarbon 51, 1111–1150.

Rempfer, J., Stocker, T.F., Joos, F., Dutay, J.C., 2012. On the relationship between Nd isotopic composition and ocean overturning circulation in idealized freshwater discharge events. Paleoceanography 27. http://dx.doi.org/10.1029/2012PA002312.

Rintoul, S.R., 1991. South Atlantic interbasin exchange. J. Geophys. Res. 96, 2675–2692.

Roberts, N.L., Piotrowski, A.M., Elderfield, H., Eglinton, T.I., Lomas, M.W., 2012. Rare earth element association with foraminifera. Geochim. Cosmochim. Acta 94, 57–71.

Roberts, N.L., Piotrowski, A.M., McManus, J., Keigwin, L.D., 2010. Synchronous deglacial overturning and water mass source changes. Science 327, 75–77.

Robinson, L.F., van de Flierdt, T., 2009. Southern Ocean evidence for reduced export of North Atlantic Deep Water during Heinrich event 1. Geology 37, 195–198.

Sabine, C.L., Feely, R.A., Gruber, N., Key, R.M., Lee, K., Bullister, J.L., Wanninkhof, R., Wong, C.S., Wallace, D.W.R., Tibrook, B., Millero, F.J., Peng, T.-H., Kozyr, A., Ono, T., Rios, A.F., 2004. The Oceanic sink for anthropogenic CO_2. Science 305, 367–371.

Schlitzer, R., 2000. Electronic atlas of WOCE hydrographic and tracer data now available. Eos Trans. AGU 81, 45.

Schmitz Jr., W.J., McCartney, M.S., 1993. On the North Atlantic circulation. Rev. Geophys. 31, 29–49.

Siddall, M., Khatiwala, S., van de Flierdt, T., Jones, K., Goldstein, S.L., Hemming, S., Anderson, R.F., 2008. Towards explaining the Nd paradox using reversible scavenging in an ocean general circulation model. Earth Planet. Sci. Lett. 274, 448–461.

Sigman, D., de Boer, M.A., Haug, G.H., 2007. Antarctic stratification, atmospheric water vapor, and Heinrich events: A hypothesis for late Pleistocene deglaciations. In: Schmittner, A., Chiang, J.H.C., Hemming, S.R. (Eds.), Past and Future Changes of the Oceanic Meridional Overturning Circulation: Mechanisms and Impacts. In: Geophys. Monogr., vol. 173, pp. 335–349.

Sloyan, B.M., Rintoul, S.R., 2001. Circulation, renewal, and modification of Antarctic mode and intermediate water. J. Phys. Oceanogr. 31, 1005–1030.

Stichel, T., Frank, M., Rickli, J., Haley, B.A., 2012. The hafnium and neodymium isotope composition of seawater in the Atlantic sector of the Southern ocean. Earth Planet. Sci. Lett. 317–318, 282–294.

Tachikawa, K., Toyofuku, T., Basile-Doelsch, I., Delhaye, T., 2013. Microscale neodymium distribution in sedimentary planktonic foraminiferal tests and associated mineral phases. Geochim. Cosmochim. Acta 100, 11–23.

Talley, L.D., 1999. Some aspects of ocean heat transport by the shallow, intermediate and deep overturning circulation. In: Clark, P.U., Webb, R.S., Keigwin, L.D. (Eds.), Mechanism of Global Climate Change at Millennial Time Scales. In: Geophys. Monogr., vol. 112. American Geophysical Union, pp. 1–22.

Toggweiler, J.R., Lee, D.W., 2010. Temperature differenced between the hemispheres and ice age climate variability. Paleoceanography 25, PA2212. http://dx.doi.org/10.1029/2009PA001758.

Tomczak, M., Godfrey, J.S., 1994. Regional Oceanography: An Introduction. Pergamon Press.

van de Flierdt, T., Robinson, L.F., Adkins, J.F., Hemming, S.R., Goldstein, S.L., 2006. Temporal stability of the neodymium isotope signature of the Holocene to glacial North Atlantic. Paleoceanography 21, PA4102. http://dx.doi.org/10.1029/2006PA001294.

van de Flierdt, T., et al., 2012. GEOTRACES intercalibration of neodymium isotopes and rare element concentrations in seawater and suspended particles. Part I: Reproducibility of results for the international intercomparison. Limnol. Oceanogr., Methods 10, 234–251.

Vellinga, M., Wood, R.A., 2002. Global climatic impacts on a collapse of the Atlantic thermohaline circulation. Clim. Change 54, 251–267.

White, W.M., Dupré, B., Vidal, P., 1985. Isotope and trace element geochemistry of sediments from the Barbados Ridge–Demerara Plain region, Atlantic Ocean. Geochim. Cosmochim. Acta 49, 1875–1886.

Wilson, D.J., Piotrowski, A.M., Galy, A., Clegg, J.A., 2013. Reactivity of neodymium carriers in deep-sea sediments: Implications for boundary exchange and paleoceanography. Geochim. Cosmochim. Acta 109, 197–221.

Wilson, D.J., Piotrowski, A.M., Galy, A., McCave, I.N., 2012. A boundary exchange influence on deglacial neodymium isotope records from the deep western Indian Ocean. Earth Planet. Sci. Lett. 341–344, 35–47.

Xie, R.C., Marcantonio, F., Schmidt, M.W., 2012. Deglacial variability of Antarctic intermediate water penetration into the North Atlantic from authigenic neodymium isotope ratios. Paleoceanography 27, PA3221. http://dx.doi.org/10.1029/2012PA002337.

Yu, J.M., Elderfield, H., Piotrowski, A.M., 2008. Seawater carbonate ion-$\delta^{13}C$ systematics and application to glacial–interglacial North Atlantic ocean circulation. Earth Planet. Sci. Lett. 271, 209–220.

Zhang, R., Delworth, T.L., 2005. Simulated tropical response to a substantial weakening of the Atlantic thermohaline circulation. J. Climate 18, 1853–1860.